12.5. USE OF HIGH-RESOLUTION WRF SIMULATIONS TO FORECAST LIGHTNING THREAT

Eugene W. McCaul, Jr.*, Universities Space Research Association, Huntsville, AL
Kate LaCasse, University of Alabama in Huntsville, Huntsville, AL
Steven J. Goodman, NASA Marshall Space Flight Center
Daniel Cecil, University of Alabama in Huntsville, Huntsville, AL

1. INTRODUCTION

Accurate forecasts of the lightning threat are desired by many components of the military, business and recreational communities. Previous attempts to provide prognostic guidance on the lightning threat have tended to focus either on point forecasts (Mazany et al. 2002) or area-wide forecasts (Bright et al. 2004; Burrows et al. 2005), and have been typically based on observations and indices previously found to be associated with convective storm activity.

In recent years, research has shown there to be strong relationships between observed lightning flash rates and the occurrence of precipitation-size ice hydrometeors in the mixed phase regions of storm updrafts (Cecil et al. 2005; Petersen et al. 2006). Many operational numerical models now have the ability to be run at sufficiently high resolution to represent individual convective storms and their ice microphysical properties explicitly. The increasing availability of such models offers the opportunity to explore the possibility of forecasting lightning threat using appropriate kinematic and microphysical fields generated by the model simulations.

In this paper, we present preliminary results from a series of mesoscale cloud-resolving simulations using the Weather Research and Forecasting (WRF) Model (Skamarock et al. 2005), in which we assess the utility of the model in producing short-term forecasts of the time-dependent, space-dependent lightning threat over the Tennessee Valley region. Although the WRF model does not yet contain explicit electrification algorithms, it produces several fields that, taken together, can be considered proxies for electrification processes. In this paper, the lightning threat is estimated using two proxy methods, one based on the simulated microphysical fields, the other on the simulated reflectivity structure. Ground-based total lightning data and NWS Doppler radar data are available as ground truth for the simulated fields in our case studies.

2. METHODOLOGY

Based on the recent work by Petersen et al. (2006) and Cecil et al. (2005) we propose the use of two proxies for storm electrification processes that lead to lightning: (1) a flash rate field that is proportional to the simulated convective-scale upward fluxes of graupel (see Petersen et al. 2006), and (2) a flash rate field derived from linear regression of satellite-observed flash rates against satellite-observed vertical radar reflectivity values in the mixed and ice phase portions of the convective clouds (see Cecil et al. 2005). The satellite-based lightning and reflectivity data are obtained from the Lightning Imaging Sensor (LIS) and the Precipitation Radar (PR) on board the polar-orbiting Tropical Rainfall Measuring Mission (TRMM) platform. The simulation-based threat fields and reflectivity fields are then compared to gridded observations of lightning flash rates as measured by the North Alabama Lightning Mapping Array (Rison et al. 1999; Krehbiel et al. 2000; Koshak et al. 2004) and NWS Doppler radar observations.

The regression of LIS flash rates against PR reflectivity structure is based on the data used by Cecil et al. (2005), subsetted over the southeastern United States. Only warm season data were used, in order to obtain statistically reliable sample sizes. PR reflectivity structure was examined in many ways, but results presented here are based on reflectivity values at 6 km and 9 km. This two-level approach yielded near-optimum results without adding too much complexity to the flash rate estimation algorithm. The regression process led to the following formula for flash rate F (flashes/min/typical feature area):

$$F = aR_6 + bR_9 + c \tag{1}$$

where R_6 is reflectivity at 6 km, R_9 is reflectivity at 9 km, and the coefficients a, b and c assume numerical values of 1.0855828, 0.51961653 and -49.49, respectively. During the warm season, the 6 km reflectivity occurs at temperatures near -15C. We assume that the reflectivity results at 6 km are tied to temperature, such that for extension to the cool season, we consider a, b and c from (1) to apply to the altitudes where -15C occurs, and 3 km above that, respectively. Because the flash rates catalogued by Cecil et al. (2005) refer to storm systems of varying size, not constant gridbox sizes, the flash rates derived from (1) must be rescaled, or interpreted to refer to areas generally larger than the mesh gridboxes utilized in our cloud-resolving model. The fact that the storm systems identified by Cecil et al. (2005) exhibit a spectrum of sizes makes this rescaling a challenging task, which is an ongoing area of investigation. Our present flash rate estimates from (1) must therefore be viewed as only rough approximations. The same holds true for our flash rate estimates based on graupel flux.

*Corresponding author address: E. W. McCaul, Jr., Universities Space Research Association, 6700 Odyssey Drive, Suite 203, Huntsville, AL 35806, e-mail: mccaul@space.hsv.usra.edu

Both our flash rate prediction algorithms are based on variables output or inferred from WRF model simulation data. The WRF simulations were conducted on a 2 km x 2 km native grid covering the southeastern U. S., initialized at either 00 UTC or 12 UTC on selected case study dates, and lasting 6-12 h. The model contained 52 levels on a constant 500 m vertical mesh. The time step used in the simulations was 12 s, and 25 history times were saved, at time intervals ranging from 15 min for the 6-h simulations, to 30 min for the 12-h simulations. The shorter 6-h simulations were used for cases where convection peaked shortly after model initialization, while the 12-h simulations were used for cases of afternoon summer storms that peaked more than 8-h after model initialization. In one case, to be discussed in Results, we performed an 8-h simulation, with model saves taken at 20-min intervals. Model output was interpolated to a latitude-longitude grid with grid spacing of roughly 0.009 degrees, or about 1 km, for analysis and plotting. The WRF initial and boundary conditions were from ETA model analyses, with the addition of ACARS, METAR, and NWS Doppler radar fields at t = 0. Two sets of simulations were generated for each case, one with only Doppler radar velocity fields used, and the other with both velocity and reflectivity fields used. The WRF single moment, six-species microphysics (WSM6) package was used to represent clouds and their hydrometeors. This package allows simulation of only one large precipitating ice species, which we have characterized as graupel.

Although many case studies have been performed, we present here the results from only two. The first is a spring season severe weather outbreak that featured tornadic supercells early on 30 March 2002. This case involved storms that produced very high lightning flash rates. The second is a strongly contrasting winter case, featuring small but severe hailstorms triggered by instability associated with a cold vortex at midlevels. For this winter case, flash rates were much smaller. For both cases, total lightning flash rates were tallied using data from the North Alabama Lightning Mapping Array (LMA; (Rison et al. 1999; Krehbiel et al. 2000; Koshak et al. 2005), and were used as "ground truth" against which the simulated lightning threat products could be calibrated and compared. The LMA-derived flash rate fields were accumulated over 5-min intervals and gridded to the same mesh as that used for analysis and display of the WRF fields.

3. RESULTS AND DISCUSSION

Early on 30 March 2002, a strong cold front approached the Tennessee Valley and triggered a broken line of severe storms, with a small cluster of intense supercells breaking through a prefrontal capping inversion just south of the Tennessee River in northern Alabama. Values of convective available potential energy (CAPE) inferred from the WRF fields approached or exceeded 3000 J/kg across north Alabama when the convection began just after 00 UTC. Just after 0400 UTC, one of the supercells produced a tornado near Albertville, AL. The supercells were very strongly electrified, with flash rates on the order of 100/min, as suggested by Fig. 1a, a plot of LMA-derived gridded source density from 0400 UTC. The NWS Doppler radar-derived low-level reflectivity plot for the same time is given in Fig. 1b.

The WRF simulation, initialized at 00 UTC 30 March with Doppler velocity data but not reflectivity, also produced a broken line of strong storms, with a few isolated cells ahead of the main line. By 0400 UTC, WRF's strong updrafts generated considerable graupel, and the WRF-derived lightning threat based on graupel flux was significant and widespread, as seen in Fig. 1c. WRF reflectivities in the storm cores were also easily in excess of what might be expected to be associated with lightning, and the threat based on the two-layer reflectivity regression also suggests considerable lightning activity (Fig. 1d). WRF does a good job of depicting the broken squall line draped across much of Tennessee, but is not intense enough with the isolated storms in northeast Alabama. These latter storms are also too far northeast of their actual locations. Another WRF simulation (not shown) initialized with radar reflectivities provides no improvement for these isolated prefrontal cells, presumably because they did not develop until after the 00 UTC initialization time, and thus were not depicted in the initial reflectivity data.

A contrasting environment case is associated with the storms that occurred in the Tennessee Valley region just after 18 UTC on 10 December 2004. These storms developed beneath a core of very cold air at midlevels, with temperatures at the surface barely reaching 15C. WRF-derived CAPE values at about the time of storm initiation reached almost 600 J/kg in east-central Tennessee, a little less than the 761 J/kg observed at Huntsville by the UAH Mobile Integrated Profiling System sounding system. To study these storms, we performed an 8-h WRF simulation initialized at 12 UTC on 10 December, with data saved every 20 min. These winter storms were smaller, shallower and weaker than the storms shown in Fig. 1, but still managed to generate 2.5 cm hail and some lightning. LMA-derived source density for 1900 UTC (Fig. 2a) indicates a few low-flash rate cells in northeast Alabama, with a few other mildly electrified cells in east-central Tennessee. NWS Doppler radar-derived reflectivity maps (not shown) show numerous small, weak cells, with a few small, stronger cores having peak reflectivities near 60 dBZ.

The WRF simulation of this case captures well the timing, location, small size and scattered character of these storm cells. The simulated storms built tops to 6-7 km in reflectivity, with updrafts briefly reaching 6-10 m/s and some graupel aloft. Lightning threat based on graupel flux at -15C indicates only a few small cores capable of producing low flash rates (Fig. 2b), quite similar to observations. The simulated storms had peak reflectivities of 51 dBZ, with 50 dBZ cores sometimes reaching 4.25 km altitude. However, the simulated storms were devoid of reflectivity 3 km above

the -15C level. Thus, their reflectivity-based lightning threat was also confined to a few small, isolated cells (not shown), with small flash rates.

The results of the simulations reveal some of the capabilities of the WRF model, and also some of its limitations. While the model often produces storms at about the right time and location and intensity, it also sometimes produces unrealistically complex arrangements of storms, and excessive numbers of storms. This kind of error may be a reflection of the growth of errors that were present in the model initial state. The model simulation of the 10 December 2004 storms also showed deficiencies in peak reflectivities, and apparently also peak updraft speeds. The peak reflectivities from the archive of 20-min saves of model output yielded values only near 51 dBZ, whereas radar data indicated values reaching closer to 60 dBZ. WRF peak updrafts were only 6-10 m/s, which probably would not have been sufficient to account for the 2.5 cm hailstones that were observed at the surface. WRF's WSM6 scheme, of course, does not have the capability of representing both graupel and hail simultaneously. However, idealized simulations made using another cloud model with more advanced cloud physics and more ice species, on a 500 m horizontal mesh, gave peak reflectivities of 59 dBZ, peak updrafts of 19 m/s, and hail reaching the surface. These latter results are likely much closer to reality than the corresponding results from WRF.

4. SUMMARY AND OUTLOOK

The WRF simulations generally do a satisfactory job of generating deep convection in roughly the right places and times as observed. There are instances, however, where the model exhibits phase errors in the locations of convective storms or systems, sometimes producing too much convection as compared with observations. Despite the simplicity of the model's physics, and the coarseness of the model mesh, characteristics of the simulated storms are often adequate to suggest the presence of lightning in cases where it is observed. Furthermore, the WRF-derived lightning threat fields demonstrate a clear ability to distinguish higher flash rate cases from lower rate cases. In addition, the WRF simulations also capture the areal coverage of the evolving lightning threat with some fidelity, something which operational lightning forecast schemes based upon parameters such as CAPE cannot do; in most cases, only a small fraction of the area having positive CAPE is actually experiencing storms at any given instant. Furthermore, the WRF-based lightning threat schemes described here also provide quantitative guidance about flash rates, information which is not easily obtained from other schemes (see e.g., Bright et al. 2004). While precise quantitative calibration of the WRF-predicted flash rates is challenging, the WRF-derived lightning threat products presented here appear to be competitive with, if not actually superior to, currently available lightning forecast products. We believe there is ample evidence of the desirability of continued exploration of lightning forecast schemes using models such as WRF.

There are several areas in which the WRF simulations could benefit from additional research and development. Perhaps the most significant involves improvement in the quality and accuracy of the initial and boundary condition fields. Assimilation of additional radar and satellite fields should be useful for this purpose. The model would also benefit from incorporation of more refined ice microphysics schemes featuring additional hydrometeor categories. The addition of an explicit cloud electrification scheme is an obvious candidate for a microphysics enhancement that would permit more detailed evaluation of lightning threat. Finally, as computing power advances, use of finer model meshes than the 2 km mesh used here would also improve the fidelity of the representation of convective systems.

5. REFERENCES

Bright, D. R., M. S. Wandishin, R. E. Jewell, and S. J. Weiss, 2004: A physically based parameter for lightning prediction and its calibration in ensemble forecasts. Preprints, 22nd Conf. Severe Local Storms, Hyannis, MA, Amer. Meteor. Soc., paper 4.3.

Burrows, W. R., C. Price, and L. J. Wilson, 2005: Warm season lightning probability prediction for Canada and the northern United States. Wea. Forecasting, 20, 971-988.

Cecil, D. J., S. J. Goodman, D. J. Boccippio, E. J. Zipser, and S. W. Nesbitt, 2005: Three years of TRMM precipitation features. Part I: Radar, radiometric, and lightning characteristics. Mon. Wea. Rev., 133, 543-566.

Koshak, W. J., R. J. Solakiewicz, R. J. Blakeslee, S. J. Goodman, H. J. Christian, J. M. Hall, J. C. Bailey, E. P. Krider, M. G. Bateman, D. J. Boccippio, D. M. Mach, E. W. McCaul, M. F. Stewart, D. E. Buechler, W. A. Petersen, and D. J. Cecil, 2004: North Alabama Lightning Mapping Array (LMA): VHF source retrieval algorithm and error analyses. J. Atmos. Oceanic Technol., 21, 543-558.

Krehbiel, P.R., R.J. Thomas, W. Rison, T. Hamlin, J. Harlin, and M. Davis, 2000: GPS-based mapping system reveals lightning inside storms. EOS, 81, 21-25.

Mazany, R. A., S. Businger, S. I. Gutman, and W. Roeder, 2002: A lightning prediction index that utilizes GPS integrated precipitable water vapor. Wea. Forecasting, 17, 1034-1047.

Petersen, W. A., H. J. Christian, and S. A. Rutledge, 2005: TRMM observations of the global relationship between ice water content and lightning. Geophys. Res. Lett., 26 July 2005, vol. 32, no. 14, L14819 paper no. 10.1029/2005GL023236.

Rison, W., R. J. Thomas, P. R. Krehbiel, T. Hamlin, and J. Harlin, 1999: A GPS-based three-dimensional lightning mapping system: Initial observations in central New Mexico. Geophys. Res. Lett., 26, 3573-3576.

Skamarock, W. C., J. B. Klemp, J. Dudhia, D. O. Gill, D. M. Barker, W. Wang, and J. G. Powers, 2005: A description of the Advanced Research WRF Version 2. NCAR Technical Note NCAR/TN-468+STR, 100 pp.

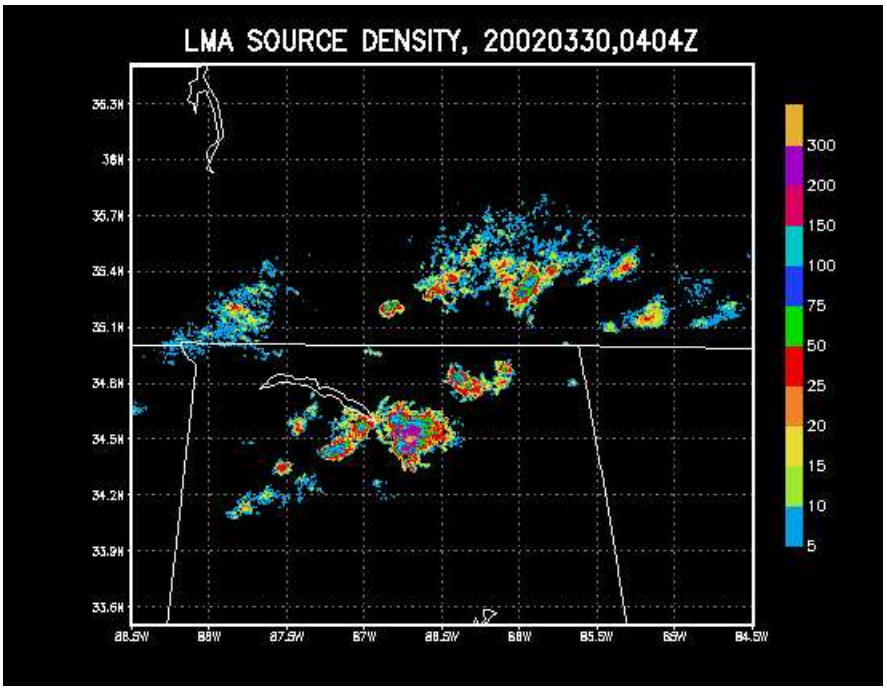

Fig. 1a. LMA-derived gridded field of source density for 04 UTC 30 March 2002.

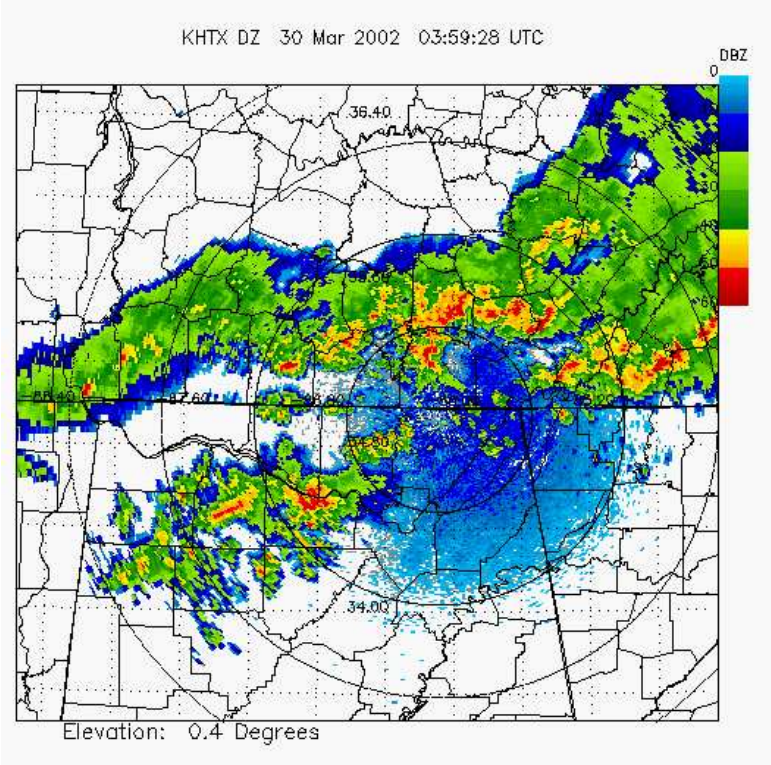

Fig. 1b. Low-level reflectivity at 0359 UTC 30 March 2002 from Hytop, AL, NWS WSR88D Doppler radar.

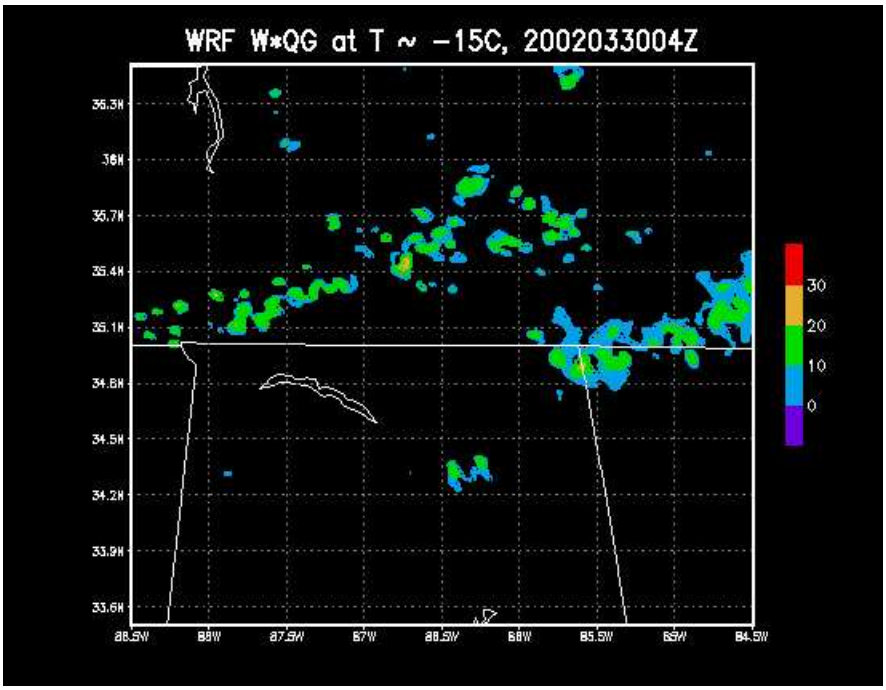

Fig. 1c. Field of WRF-derived lightning threat at 04 UTC on 30 March 2002, based on simulated graupel flux at the altitude where ambient temperature is -15C.

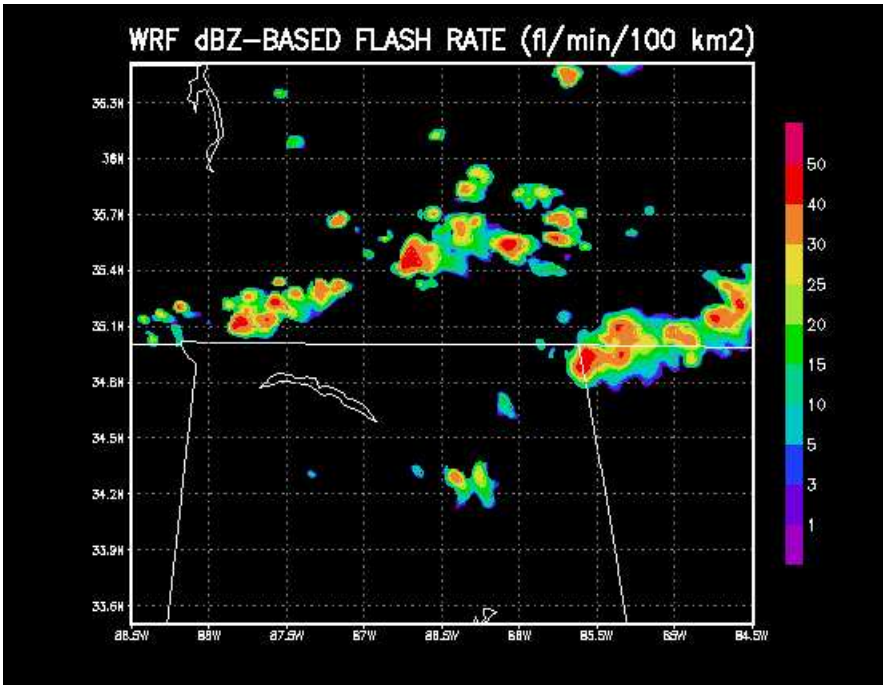

Fig. 1d. Field of WRF-derived lightning threat at 04 UTC on 30 March 2002, based on a regression of LIS flash rate against two levels of TRMM PR reflectivity applied to two comparable levels of WRF reflectivity.

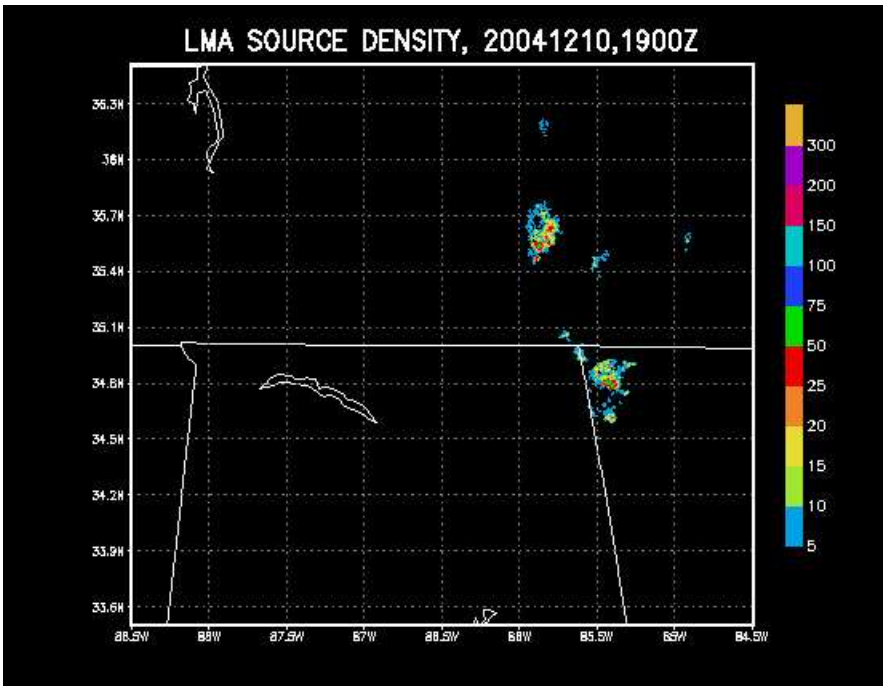

Fig. 2a. LMA-derived gridded field of source density for 19 UTC 10 December 2004.

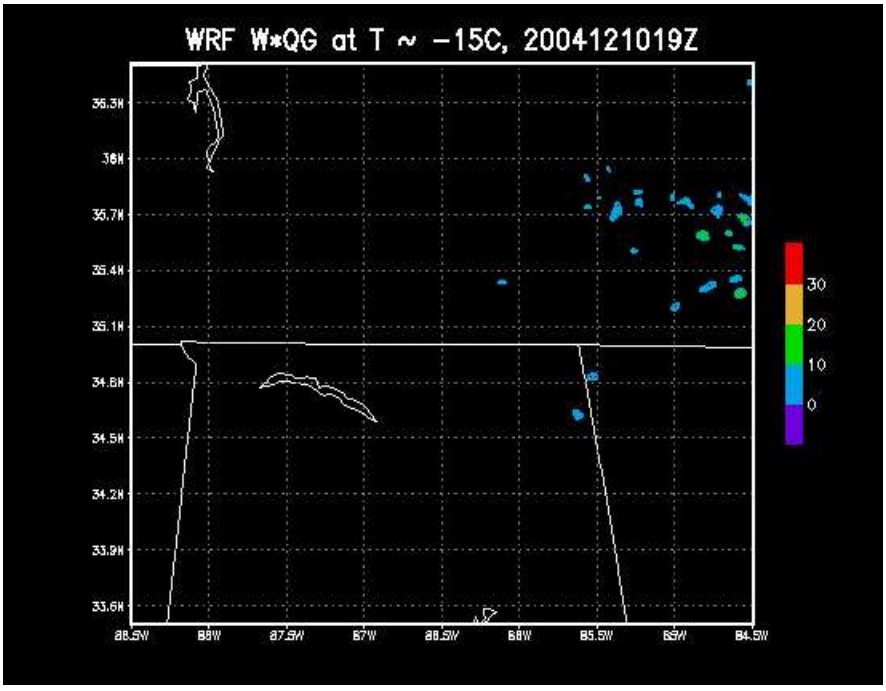

Fig. 2b. Field of WRF-derived lightning threat at 19 UTC on 10 December 2004, based on simulated graupel flux at the altitude where ambient temperature is -15C.